# Building and Registering Parameterized 3D Models of Vessel Trees for Visualization during Intervention *

Georg Langs[abc], Petia Radeva[a], David Rotger[a], Francesc Carreras[d]

[a]Computer Vision Center,
Universitat Autònoma de Barcelona, Bellaterra, Spain
{petia,rotger}@cvc.uab.es

[b]Pattern Recognition and Image Processing Group
Vienna University of Technology, Vienna, Austria
langs@prip.tuwien.ac.at

[c]Insitute for Computer Graphics and Vision
Graz University of Technology, Graz, Austria

[d]Hospital St. Pau, Barcelona, Spain
fcarreras@hsp.santpau.es

## Abstract

*In this paper we address the problem of multimodal registration of coronary vessels by developing a 3D parametrical model of vessel trees from computer tomography data and registering it to angiography images during intervention.Thus, the interventionist takes profit from 3D data otherwise only available before the intervention. This facilitates orientation in ambiguous radiographs, interactive visualization of all vessel structures to estimate their mutual position and navigation within the vessel system and ultimately reduces the radiation the patient and the physicians are exposed to.*

*The model is build by exploring the branching vessel tree starting from a single position and successively expanding through the vessels guided by a local deformable surface. The result is a tree of cylindrical segments each adapted to the vessel walls that is registered to angiography images in a fast and robust way. Validation on 8 patients confirms the robustness of our method.*

## 1 Introduction

Recently a number of new technologies to capture 3D data have been developed for medical applications. Last developments in Computer Tomography (CT) made possible to reconstruct volume data even for moving objects like the heart. The 3D information now available is crucial not only for the planning of interventions but also to guide the intervention itself. Currently different angiographic projections are used to monitor the operation of a catheter in the coronary artery tree during interventional radiology procedures. They provide only 2D data and hence make navigation difficult resulting in frequent repositioning of the image intensifier tube during the procedure, to select the most appropriate radiologic projection and to avoid vessel superimpositions. Registration of CT to X-ray images of coronary vessels will allow to overcome the disadvantages of intraoperative X-ray images: low image contrast, difficult and ambiguous interpretation of vessels due to the overlapping nature of radiographs and measurement distortion, by the advantages of preoperative (CT) data: high image contrast, complete and true 3D reconstruction of vessels and real measurements.

The importance of registration of CT to X-Ray images has been noted by several authors as a valuable tool to provide a complete and high quality 3D information in addition to the poor data provided by X-ray images. Different approaches can be clustered as image-based [7] and geometry-based registration [11, 6]. In general, geometry-based registration has the advantage of being faster, more robust and allows an interactive display of 3D models and image data. Geometry-based registration contains different subproblems to be addressed: 3D reconstruction from volumetric (CT) images, 2D segmentation of X-ray image (optional), calibration of the X-ray system and registration and visualization of 3D models to X-Ray 2D data.

One of the basic novelties of this paper is that we address most of these problems in order to perform registration of coronary vessels that are highly deformable physical structures organized in a coronary tree often having an ambiguous projection in the X-ray image due to their overlapping and measurement distortion. We propose an approach to make the 3D information available during the cardiac catheterization procedure by building a physics-based model of the vessel tree and registering it to the angiography image. This enables the physician not only to navigate more easily through the branching vessels with the help of an explicit model but makes planning of angiographic projections possible in advance. It facilitates intervention guidance and spares the patient additional exposure to radiation.

Different approaches to segment 3D data exist. In [1] vessel trees and medial axes are extracted by applying a morphological method. Deformable models are widely used in medical applications due to their robustness and the resulting explicit description of the entity of interest [9]. In [2, 4] a minimal cost path algorithm is used to perform an active contour search between two given points.

*This research has been supported by the Austrian Science Fund (FWF) under the grants P17083-N04, P14445-MAT and P14662-INF.

In [8] deformable organisms were introduced. They are autonomous agents, that perform the subsequent segmentation steps based on internal information and a sensory unit, that is aware of parts of or the entire data.

In this work we adopted a physics-based approach by exploring the vessel system with a local deformable model in order to successively build a parametric model of the vessel tree consisting of cylindrical segments. The 3D model is registered to the X-ray image making possible an interactive visualization of the 3D model and multimodal (CT and X-ray) data.

The two parts are fairly independent. The 3D model can be used for other purposes like inspection of the vessel before intervention or can be derived from other data like 3D magnetic resonance angiogram images. The registration can be applied as well to the entire CT volume in order to visualize other structures not visible in angiography.

The paper is organized as follows: the building of a vessel tree model is explained in Sec.2. In Sec.3 the registration during intervention is described. Experimental results are presented in Sec.4 and a conclusion is given in Sec.5.

## 2 A physics-based model for 3D reconstruction of vessels from CT

The first part of the algorithm builds a 3D model of a branching vessel structure based on CT data. Starting from a single point and a direction in the CT-volume the search for the vessel structure proceeds in a local manner. It spreads through the vessel system necessary to be visualized during intervention. It happens before intervention and results in a model of the vessel tree consisting of cylindrical segments adapted to the shape of the true vessels.

Although the method has been developed with the application on vessels in mind it is fitted to any branching structure with long tubular segments. Branchings and initialization positions for travels along a vessel segment are detected automatically, it can be viewed as an extension to standard snakes similar to deformable organisms [8] in 3D. It is therefore expandable within the same framework.

**Vessel enhancement filtering** To support the building of the vessel model a vesselness enhancement filter is applied to the CT data $\mathbf{I}^{CT}$. In [5] an approach to filter Magnetic Resonance angiography volumes to detect tubular structures was introduced. The filter results in a *vesselness value* that is used to weight the original volume resulting in the enhanced data $\mathbf{I}$.

**The deformable model** The model of the vessel tree is built in a local manner. A deformable surface initialized as a circle with given position $\mathbf{P}_1$ , radius $r_1$ and orientation $\mathbf{d}_1$ is used as *explorer balloon*. It is inflated by a directed pressure force. After convergence the next position of the medial axis, the radius and the direction are derived from the surface and a new explorer balloon is initialized. The *organism* moves through the vessel tree utilizing the explorer balloon as sensor and a simple memory of its path. Fig.1(a) shows a scheme of the system. The deformable model formulation used in this work follows [9], finite element based solutions in 2D and 3D are explained in detail in [3]. In the following only a short overview is given.

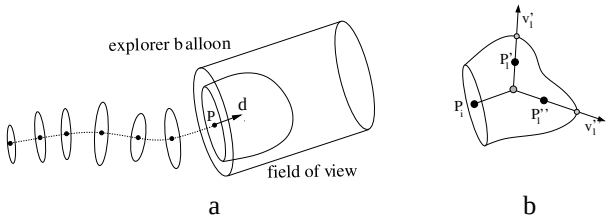


**Figure 1. (a) Scheme of the local deformable model, the field of view, vessel medial axis and radius estimates. (b) Initializing two segments at a branching.**

The parameterized surface $\mathbf{x}(s,r) = (\mathbf{x}_1(s,r), \mathbf{x}_2(s,r), \mathbf{x}_3(s,r))$, moves through the 3D-volume by minimizing an energy functional $E(\mathbf{x})$ depending on internal and external forces. The external forces derived from the 3D data $\mathbf{I}(x,y,z)$ constitute the potential $P_{ext}$. The internal energy is determined by parameters establishing elasticity, rigidity and resistance against twist of the surface. Boundary conditions may be introduced and the resulting surface can be interpreted as a thin plate. Further steering possibilities are introduced by a directed pressure force

$$F_{pr} = k_1\mathbf{n}(r,s) + k_2\mathbf{d}, \tag{1}$$

where $\mathbf{n}$ is the normal vector on the surface in the parameter position $(r,s)$ and $\mathbf{d}$ is a direction used to make the model move through the vessel.

### 2.1 Local building process

**A step forward** The building procedure starts from a given position $\mathbf{P}_i$ in the direction $\mathbf{d}_i$. The deformable surface is initialized as a triangular mesh filling a circle with radius $r_i$. During the deformation of the surface the energy functional $E = E_{int}+E_{ext}+E_{pr}$ is minimized. During this work $E_{ext}$ is the gradient information based on a part of the filtered CT volume data $\mathbf{I}$ thresholded at a value corresponding to the expected Hounsfield number within the vessels after contrast fluid has been applied. On the resulting data a distance transform is performed resulting in $\mathbf{I}^d$ and a corresponding *distance potential force field* [3] $E_{ext} = -|\nabla\mathbf{I}^d|^2$.

Only a part of the entire data, the *field of view*, is used for the deformation of the explorer balloon. This focuses the optimization on a region where substantial progress can be expected.

$E_{int}$ is established by internal mechanical properties of the surface as described above, and $E_{pr}$ is determined by the force in Eq.1. After the optimization procedure for the deformable model has converged new values for an initialization circle can be derived from the resulting surface.

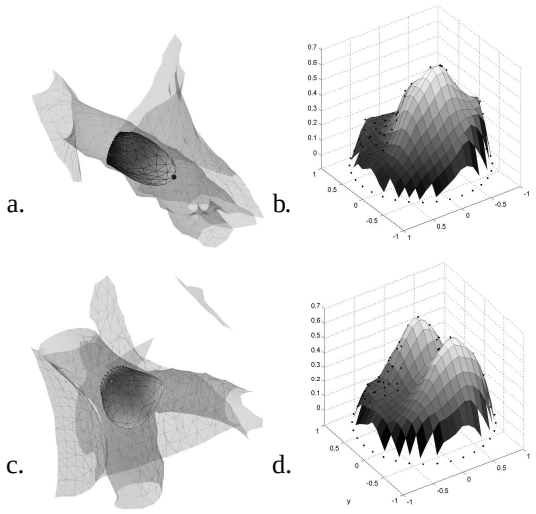


**Figure 2. Explorer head and corresponding curvature values: upper row: within a vessel, lower row: detecting a vessel bifurcation**

**New $\mathbf{P}$, $\mathbf{v}$ and $\mathbf{r}$** Given the points of the surface $(\mathbf{x}_k)_{k=1\ldots,K}$, with $\mathbf{x}_k \in \mathbb{R}^3$ the new values are

$$\mathbf{P}_{i+1} = mean_{k=1\ldots,K}(\mathbf{x}_k), \quad (2)$$

$$\mathbf{v}_{i+1} = (\mathbf{P}_{i+1} - \mathbf{P}_i)/\|\mathbf{P}_{i+1} - \mathbf{P}_i\| \quad \text{and} \quad (3)$$

$$\mathbf{r}_{i+1} = mean_{k=1\ldots,K}(dist(\mathbf{x}_k, \overline{\mathbf{P}_i\mathbf{P}_{i+1}})). \quad (4)$$

The values $\mathbf{r}_i$ are coarse estimates of the radius values of the vessel at positions $\mathbf{P}_i$. For initialization of the circular surface in the following step a slightly smaller value proved to give better results. Still for the final fitting of a cylindrical model to the vessel the values $\mathbf{r}_i$ are used.

**Detection of bifurcations** The internal energy $E_{int}$ can also be used to determine local information on the curvature of the surface. Fig.2 shows explorer balloons (a) within a vessel and (c) confronting a bifurcation in the vessel structure, in Fig.2(b) and (d) local curvatures of the surfaces are plotted over the surface parameterization. Multiple local maxima can be used as indicator for branchings. Thereby the balloon serves as a local bifurcation detector within the vessel. A second surface with higher resolution and an independent parameter set is used to verify the bifurcation, allowing for control of the detectors sensitivity. After detecting a bifurcation the present vessel segment is ended and new vessel segments are initialized according to the local maxima of

$$c_{loc}(r,s) = \|\frac{\delta^2\mathbf{x}}{\delta r^2}\| + \|\frac{\delta^2\mathbf{x}}{\delta r \delta s}\| + \|\frac{\delta^2\mathbf{x}}{\delta s^2}\| \quad (5)$$

In Fig.1(b) an explorer head at position $\mathbf{P}'_i$ detects a bifurcation, two new segments with positions $\mathbf{P}'_1$ and $\mathbf{P}''_1$ and directions $\mathbf{v}'_1$ and $\mathbf{v}''_1$ start at the vessel branching. The previous sequence of medial axis points $(\mathbf{P}_i)_{i=1,\ldots,i_{fin}}$ and corresponding radius values $(\mathbf{r}_i)_{i=1,\ldots,i_{fin}}$ is subject to further refinement described later on.

If a vessel passes the border of the data cube, is not filled with contrast fluid or when its diameter decreases below the resolution of the CT data, the vessel segment is finished without succeeding branches.

**Pruning of vessel segments** Sharp turns of vessels or branches not sufficiently filled with contrast fluid can result in false bifurcations and two explorer heads traveling along the same vessel. The memory of detected medial axes and radius values during vessel building allows for an immediate pruning of multiple vessel segments. Exploring of segments is stopped if for a new position $\mathbf{P}$: $\|\mathbf{P} - \mathbf{P}'_i\| < r'_i$ holds for any $\mathbf{P}'_i$ part of the existing vessel segments.

**Fitting the model to single vessel segments** For each vessel segment a cylindrical deformable surface is fitted to the 3D data. It is initialized with the estimates obtained by the explorer balloon and results in a final approximation of the vessel medial axis and walls. Again the standard snake method is used.

### 2.2 Merging the segments to a vessel tree

The resulting model of the vessel tree consists of a set of vessel segments $(\mathbf{V}_i)_{i=1,\ldots,N}$ and a set of bifurcations $(\mathbf{B}_i)_{i=1,\ldots,M}$. Each Vessel segment holds coordinate information about the vessel medial axis and a surface representing the vessel wall. The bifurcations $V_i$ hold their coordinates, the indices of the incoming vessel segment and the indices of the outgoing segments.

## 3 Registration and visualization during intervention

In the second step the 3D model is registered to an angiography during a diastolic phase after contrast fluid has been injected during a catheter intervention. The transformation is calculated based on known parameters of the positioning devices and two manually indicated points.

Two points are marked in the 3D model and on the angiography. Usually bifurcation points are used. The registration is based on the known angles $\alpha$ and $\beta$ of the angiography device positioner, the points in the volume and the angiography providing information about the angle $\gamma$ and the translation of the patient during intervention. The rotation and scaling matrix $\kappa R(\alpha, \beta, \gamma)$ and two translations $T_1$ and $T_2$ can be calculated to transform coordinates in the CT system $x^{CT}$ to the corresponding coordinates in the angiography system $x^{ang}$ by $x^{ang} = \kappa R(x^{CT} - T_1) + T_2$. The scaling accounts for voxel and pixel sizes. $T_2$ can be chosen either by estimating the distance of the vessel to the image plane based on the two manually indicated points or to let the model lie close to the image plane which proved to be better suited for visualization purposes. The resulting registered model is visualized together with the angiography so that interventionists are able to rotate and translate the pair arbitrarily.

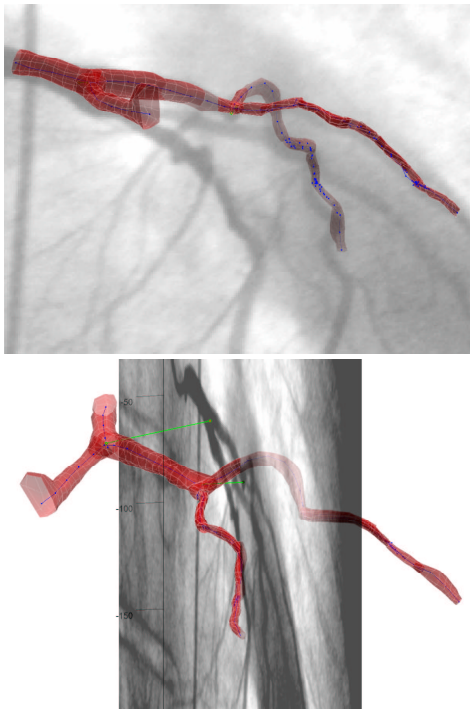

**Figure 3. Registered vessel model.**

## 4 Results

To evaluate our approach we acquired a set of CT data of 8 patients using a Toshiba Aquilion 16 multislice scanner. Data had a spatial resolution of 0.49 $\times$ 0.49 $\times$ 0.6mm. Intraoperative X-ray images from different views of the same patients have been acquired a month later by a Philips Integris HM 3000 that provided DICOM images of size 512 $\times$ 512 pixels. Since our purpose is to obtain a fast multimodal registration of preoperative and intraoperative data in order to guide the intervention, we need the projection of 3D models to support identification of vessels in the X-ray images. Exact coincidence of vessels is impossible taking into account that vessels deform with the cardiac cycle, they depend on the respiration of the patient. Therefore, our validation procedure is based on a criterion of vessels overlapping instead of exact superposition. To diminish the effects of vessel deformation, only diastolic images have been processed. Note that in our approach time-consuming procedures of calibration of X-ray images for each view are avoided, solving the registration problem by the X-ray scanner parameters and just two anatomical landmarks identified by the physician in both image modalities. For each patient models and filtered CT volumes of the left coronary artery were registered to two X-ray images taken from different angles. The pairs provided sufficient accuracy for navigation. From the 8 patient cases due to overlapping structures in 2 cases identification of the landmarks was difficult, making an interactive procedure necessary. Calculation time for the transformation was 0.3 sec. Model building is robust against noise but can suffer from calcium saturation in CT images causing vessel structures seeming to merge. Registering models is significantly faster than registering volume data due to the decreased number of points. Fig.3 shows an angiography together with the registered model of the vessel tree under two different perspectives, that is available to the physician for interactive visualization and evaluation.

## 5 Conclusion

A method to build 3D models of branching vessel trees from CT data and registering them to angiographies during intervention was introduced. The model building process is local and starts from a single point and direction. The registration allows for the use of important 3D information obtained with new CT techniques available during intervention. Until now only 2D image sequences could be used. It makes navigation easier, angiography planning possible and thus renders the decrease of radiation exposure during intervention possible.

Future research will focus on a fastening of the model building process and the projection of a tracked catheter position in the angiography onto the model. Resulting models of the vessel tree can be object to non rigid registrations as presented in [10].

## References


[1] Z. Chen and S. Molloi. Automatic 3d vascular tree construction in ct angiography. *CMIG*, 27:469–479, 2003.

[2] L. Cohen and R. Kimmel. Global minimum for active contour models: A minimal path approach. In *CVPR*, p. 666–673, 1996.

[3] L. D. Cohen and I. Cohen. Finite element methods for active contour and ballons for 2d and 3d images. *Trans. PAMI*, 15:1131–1147, 1993.

[4] A. Frangi, W. Niessen, R. Hoogeveen, T. van Walsum, M. Viergever. Model-based quantitation of 3d magnetic resonance angiographic images. *IEEE TMI*, 18(10):946–956, 1999.

[5] A. F. Frangi, W. Niessen, K. Vincken, and M. Viergever. Multiscale vessel enhancement filtering. In *Proc. MICCAI*, number 1496 in LNCS, pages 130–137, 1998.

[6] A. Guéziec, P. Kazanzides, B. Williamson, and R. H. Taylor. Anatomy-based registration of ct-scan and introoperative x-ray images for guiding surgical robot. *IEEE TMI*, 17:715–728, 1998.

[7] A. Hamadeh, S. Lavallé, and P. Cinquin. Automated 3-dimensional computed tomographic and fluoroscopic image registration. *Comp. Aided Surg.*, 3(1), 1998.

[8] G. Hamarneh, T. McInerney, and D. Terzopoulos. Deformable organisms for automatic medical image analysis. In *Proc. MICCAI*, 2001.

[9] M. Kass, A. Witkin, and D. Terzopoulos. Snakes: Active contour models. *IJCV*, 1:321–331, 1988.

[10] C. Twining and S. Marsland. Constructing diffeomorphic representations of non-rigid registrations of medical images. In *Proc. IPMI*, LNCS 2732, pages 413–425, 2003.

[11] Z. Zhang. Iterative point matching for registration of free-form curves and surfaces. *IJCV*, 13(2):119–148, 1994.